Multilayer-relaxed structure of the (1×2) Pt(110) surface

J. I. Lee
Department of Physics, Inha University, Inchon 402-751, Korea

W. Mannstadt and A. J. Freeman
Department of Physics and Astronomy, Northwestern University, Evanston, Illinois 60208

(Received 6 July 1998)

The multilayer-relaxed structure and electronic properties of the (1×2) Pt(110) surface have been investigated by the self-consistent all-electron full-potential linearized augmented plane-wave method. The relaxed geometry, determined by total energy and atomic force calculations, shows large contractions in the first and second interlayer spacings, significant buckling in the third layer, and a lateral displacement in the fourth (center) layer of the slab. In general, our calculated results are consistent with experimental data. The microscopic origin of the relaxed structure is discussed using the calculated electronic structures. The large inward relaxation of the surface atoms is attributed to the more localized nature of their $5d$ electrons, which weakens the d-d hybridization. [S0163-1829(99)06804-6]

I. INTRODUCTION

Various experimental and theoretical investigations have confirmed that the (110) surfaces of Au and Pt exhibit (1×2) missing row structures. It is also generally accepted that (1×2) Pt(110) and (1×2) Au(110) undergo a large contraction in the first interlayer spacing, a slight row pairing in the second layer, and significant buckling in the third layer.[1–15] The low-energy electron diffraction (LEED) data analysis for the first interplanar relaxation in the (1×2) Au(110) surface gave -0.29 Å (Ref. 2) and that of x-ray diffraction (XRD) produced -0.32 ± 0.10 Å.[7] The results calculated by the embedded-atom method (EAM) (-0.21 Å)[9] and by molecular dynamics using the empirical ''glue'' Hamiltonian (-27.5%)[10] are comparable to the experimental results. The calculation by the tight-binding scheme again resulted in a smaller relaxation (-6.16%).[11] The first principles pseudopotential density-functional calculation for the (1×2) Au(110) performed by Ho and Bohnen[12] supported the LEED (Ref. 1) and ion scattering[13] experiments, but disagreed with the x-ray diffraction[16] and high-resolution electron microscopy[17] results. The situation for the (1×2) Pt(110) surface is similar to that for the (1×2) Au(110) surface.

The observed first-layer relaxation in (1×2) Pt(110), however, shows a considerable variation from -0.22 Å (-16% of the unrelaxed interlayer spacing) to -0.5 ± 0.1 Å($-36.1\pm7.2\%$): -0.26 and -0.28 Å by LEED,[2,3] -0.22 Å by medium-energy ion scattering (MEIS),[4] -0.27 Å by XRD,[7] -0.34 ± 0.04 Å by reflection high-energy electron diffraction (RHEED),[8] -0.42 Å by x-ray photoemission diffraction (XPD),[14] and -0.5 ± 0.1 Å by neutral impact collision ion-scattering spectroscopy[18] (NICISS) (cf. Table I). Contrary to experiments, the calculated results predicted rather smaller values for the first-interlayer relaxation: -7.74% by a Slater-Koster parameterized tight-binding scheme[11] and -7.4% by the linear combination of atomic orbitals (LCAO) formalism including repulsive Born-Mayer-type interactions.[19] The theoretical embedded-atom method[9,15] results, however, produced values (-0.25 Å and -0.19 Å) that are comparable to most of the experimental values. However, as far as we know, no first-principles calculations have been made on the relaxations for (1×2) Pt(110). Under these circumstances, it is very meaningful to calculate the relaxed geometry of the reconstructed systems. In this study, the multilayer relaxation in (1×2) Pt(110) is determined by the full-potential linearized augmented plane-wave (FLAPW) method[20,21] implemented with total energy and atomic force calculations and the mechanism driving the relaxed structure is discussed using the calculated electronic structures.

II. CALCULATIONAL METHOD

We model the (1×2) Pt(110) surface by a single slab consisting of seven layers (cf. Fig. 1). For the outermost surface layer on each side of the slab, the missing row (1×2) structure is assumed. The bulk lattice constant of fcc Pt is taken to be 7.407 a.u. (3.92 Å);[22] the corresponding unrelaxed interlayer spacing is then 2.619 a.u. (1.39 Å). The Kohn-Sham equations[23] incorporating the Hedin-Lundqvist exchange-correlation potential[24] are solved self-consistently

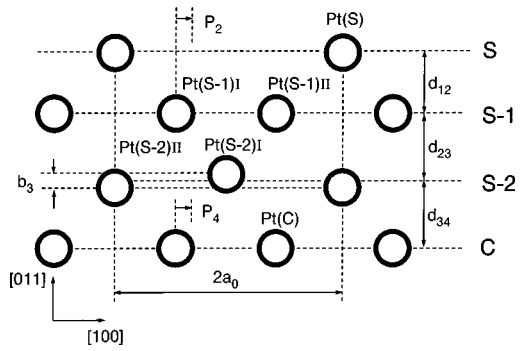

FIG. 1. Schematic drawing of the geometry of the missing-row structure for the (1×2) Pt(110) surface.

TABLE I. Comparison of the calculated relaxation of the (1×2) Pt(110) surface with various experiments and other calculations. Δd_{12} and Δd_{23} denote the relaxation of the first- and second-interlayer spacings, respectively, in Å and % (in parentheses), P_2 and P_4 represent the second-layer and fourth-layer pairing, respectively, and b_3 denotes the buckling in the third layer.

	Δd_{12} [Å (%)]	Δd_{23} [Å (%)]	P_2 (Å)	b_3 (Å)	P_4 (Å)	Ref.
LEED	-0.26 (-18)	-0.18 (-12.6)	0.065	0.320	0.120	2
LEED	-0.28 (-20)	-0.01 (-0.7)	0.04	0.17	0.05	3
MEIS	-0.22 (-16)	$+0.06$ ($+4$)	<0.04	0.10		4
RHEED	-0.37 ± 0.03 (-27 ± 2)	$+0.07\pm0.01$ ($+5\pm1$)	0.08 ± 0.01	0.18 ± 0.02		6
RHEED	-0.34 ± 0.04 (-19.5 ± 2.9)	-0.01 ± 0.05 (-0.7 ± 3.6)	0.09 ± 0.04	0.12 ± 0.05		8
XRD	-0.27 (-19.5)	-0.11 (-7.9)	0.05	0.04		7
XPD	-0.42 (-30.3)					14
NICISS	-0.5 ± 0.1 (-36.1 ± 7.2)					18
LCAO	-0.10 (-7.4)					19
Tight-binding	-0.11 (-7.74)	$+0.02$ ($+1.55$)	0.02			11
EAM	-0.19 (-13.8)	-0.06 (-4.3)	-0.06	0.08	0.06	15
EAM	-0.25 (-18.0)	-0.07 (-5)	-0.03	0.04	0.11	9
Present result	-0.24 (-17.6)	-0.007 (-0.5)	0.036	0.25	0.11	

by use of the all-electron FLAPW method. The Pt muffin-tin radius is set equal to 2.3 a.u. (1.219 Å). Inside each muffin-tin sphere, charge densities and potentials are expanded in lattice harmonics with angular momentum up to $l=8$. The core electrons, including the $5p$ states, are treated fully relativistically and the valence electrons derived from the atomic $5d,6s$, and $6p$ orbitals are treated semirelativistically,[25] i.e., dropping the spin-orbit term but keeping the other relativistic terms in the Hamiltonian.

Within the irreducible wedge of the two-dimensional Brillouin zone, eigenvalues and eigenvectors are calculated using 16 k points; the Gaussian interpolation scheme is used to perform integrations over the first Brillouin zone. Self-consistency is assumed when the root-mean-square difference between the input and output charge densities is less than 2×10^{-4} electrons/(a.u.)^3.

After obtaining the converged result for the unrelaxed geometry, the equilibrium surface geometry is optimized by total energy and atomic force calculations, which allow automatic structure optimization.[26] For each self-consistent structure, the forces on all atoms were calculated. In this process, a Broyden[27] scheme was used. A stable configuration was found when the $3n$-dimensional force vector of the system (with n atoms) is close to zero. A final relaxed structure was assumed when the force on each atom was smaller than 1.5 mRy/a.u.

III. RESULTS

We found the optimized structure of (1×2) Pt(110) in which the surface atoms [Pt(S)] move directly down into the bulk region by 0.21 Å and the atoms in the subsurface layer [Pt(S-1)I and Pt(S-1)II] move up by 0.03 Å, which makes a large contraction in the first-interlayer spacing. The atoms in the subsurface layer also have a small lateral displacement (0.036 Å) and move closer to each other. For atoms in the third layer, one atom [Pt(S-2)I] moves up and the other atom [Pt(S-2)II] moves down to make a buckling geometry. We also find a lateral displacement of the atoms in the fourth (center) layer.

From the above data, the relaxation of the first (Δd_{12}) and the second (Δd_{23}) interlayer spacings are calculated to be -0.24 Å(-17.6% of the interlayer spacing) and -0.007 Å(-0.5%), respectively. The magnitude of the fourth-layer (C) pairing P_4 is 0.11 Å and is relatively larger than that of the second-layer (S-1) pairing P_2 (0.036 Å). The magnitude of the third-layer (S-2) buckling b_3 is quite large, i.e., 0.25 Å (or 9.4 % of the interlayer spacing). These results are summarized in the last row of Table I.

A comparison of our calculated results with those of various experiments and other calculations is made in Table I. For the relaxation of the first-interlayer spacing, our result is close to those of LEED,[2,3] MEIS,[4] XRD,[7] and one RHEED (Ref. 8) experiment, and one EAM (Ref. 9) calculation. The XPD,[14] the other RHEED,[6] and recent NICISS (Ref. 18) data have larger values than ours. For the second layer relaxation, our result is close to that of the LEED experiment by Fery *et al.*,[3] but the experimental data themselves have a large variation. When considered together with the second and fourth layer displacements and the buckling in the third layer, our results are consistent, in general, with those of LEED by Fery *et al.*[3] and RHEED by Korte and Meyer-Ehmsen[8] — both in the tendency and the magnitude of the displacements.

Having established the relaxed geometry for the (1×2) Pt(110) system, we now discuss the possible mechanism behind the relaxation. For this purpose, we present in Table II the number of electrons in each MT sphere for the unrelaxed and relaxed structures. By the creation of a (1×2) reconstructed surface, there is a spilling out of electrons into the vacuum region. The spill-out charge, mostly p like, serves to alleviate the sudden discontinuity at the surface and in the missing atom region. The Pt(S-1)I and Pt(S-1)II atoms also lose considerable p electrons. With the breaking of d bonds, the d electrons are more localized at the surface atoms—as can be seen from the fact that the number of d electrons of the surface atom is increased by a small amount compared to other atoms. This makes the surface Pt(S) atoms contract down into the bulk region. The displacement of the atoms in the subsurface layer [Pt(S-1)I and Pt(S-1)II] can be easily

TABLE II. Angular momentum decomposed electronic valence charge in the muffin-tin sphere of a seven-layer (1×2) Pt(110) film for the unrelaxed and relaxed geometries.

		s	*p*	*d*	Total
Unrelaxed	Pt(S)	0.37	0.15	7.16	7.72
	Pt(S-1)I	0.37	0.20	7.15	7.75
	Pt(S-1)II	0.37	0.20	7.15	7.75
	Pt(S-2)I	0.38	0.26	7.09	7.76
	Pt(S-2)II	0.37	0.26	7.14	7.82
	Pt(C)	0.37	0.27	7.13	7.82
Relaxed	Pt(S)	0.40	0.18	7.17	7.78
	Pt(S-1)I	0.38	0.21	7.14	7.77
	Pt(S-1)II	0.38	0.21	7.14	7.77
	Pt(S-2)I	0.39	0.26	7.09	7.79
	Pt(S-2)II	0.36	0.26	7.15	7.82
	Pt(C)	0.37	0.25	7.12	7.79

understood. The subsurface atoms move close to the missing-row site to smooth the large corrugation produced by the missing rows. The net change in position for these atoms is $\Delta x=\pm0.036$ Å and $\Delta z=+0.033$ Å. With this displacement, the interplanar distance between surface and subsurface layers contracts considerably.

One also needs to notice that the atoms in the third layer, Pt(S-2)I and Pt(S-2)II have different numbers of *d* electrons. This is due to the different geometrical environment surrounding them: there is a missing-row site at the surface layer directly above the Pt(S-2)I atom. Because of the large presence of *p* electrons spilled out from surface atoms in the missing-row region, the spill out of *p* electrons from Pt(S-2)I is suppressed. Instead, the *d* electrons move out to be more delocalized and they increase the *p*-*d* hybridization with the Pt(S-1) atoms. This increased *p*-*d* hybridization makes the Pt(S-2)I atoms move up considerably ($\Delta z=+0.16$ Å) and this displacement also decreases the interplanar distance between the second and third layers. The considerable up displacement of Pt(S-2)I atoms causes a lateral displacement in the layer below. The Pt(S-2)II atoms receive repulsive forces from the contracted Pt(S) atoms, and thus they move down to the bulk region by $\Delta z=-0.08$ Å. As result of this displacement, there is a buckling ($b_3=0.25$ Å) in the third layer. The *z*-direction distance between the Pt(S) and Pt(S-2)II atoms is also decreased from its bulk value (2.772 Å) to 2.646 Å, which results in a slight increase in the hybridization between these atoms.

We consider now the density of states (DOS) associated with each atom type. The layer-by-layer DOS (LDOS) for each atom type is given in Fig. 2. As mentioned above, the creation of the surface causes greater localization of the *d* electrons in the surface layer. The width of the surface layer LDOS is decreased and the center of the *d* states shifts up compared to that of the center layer. We note here that a large peak is located at the Fermi energy, which predicts that the unrelaxed structure is unstable. After the relaxation, there is an increase in the number of *p* electrons in the MT sphere of the Pt(S) atom and the width of the LDOS is broadened. The general shape of the LDOS in each layer becomes blurred after relaxation.

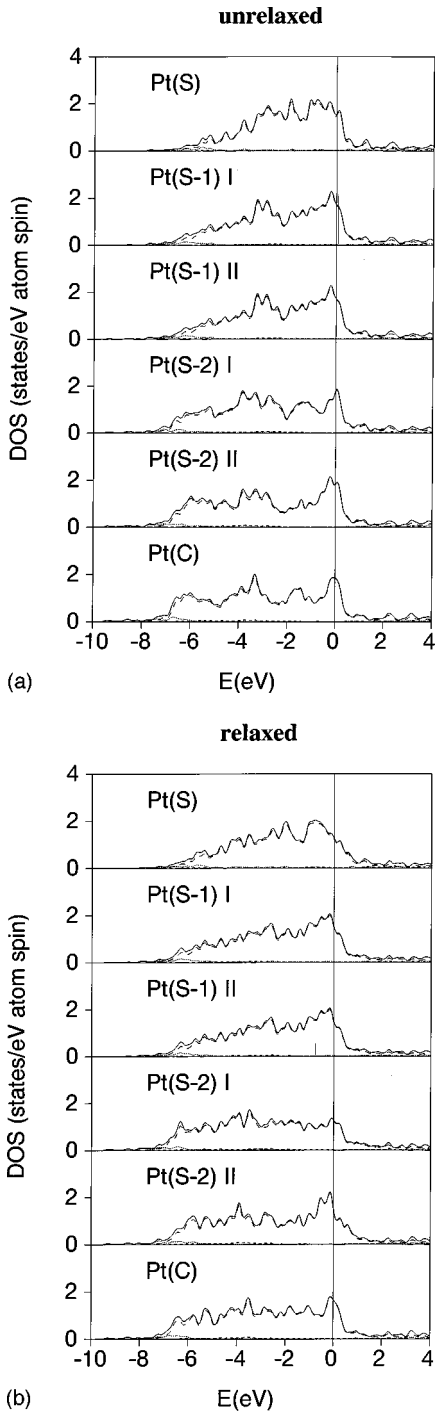

FIG. 2. Partial density of states associated with each atom type for the (a) unrelaxed and (b) relaxed (1×2) Pt(110) film, in units of states /eV atom. Dashed lines indicate *d* states, dotted lines represent *s* ($\cdots$), and dotted-dashed lines represent *p* ($-\cdot-\cdot-$) states.

IV. SUMMARY

The multilayer-relaxed structure and electronic properties of (1×2) Pt(110) have been investigated by the self-consistent all-electron full-potential linearized augmented plane-wave (FLAPW) method. The relaxed geometry, determined by total energy and atomic force calculations, shows large contractions in the first-interlayer spacing (-17.6%) and second interlayer spacing (-0.5%), and a significant buckling (0.25 Å) in the third layer. There is a lateral dis-

placement in the fourth (center) layer. Our calculated results are consistent with those of many experiments, especially those of LEED by Fery *et al.*,[3] but not with some experiments.

The microscopic origin of the relaxed structure was discussed using the calculated electronic structures, i.e., the number of electrons in MT spheres and the layer-by-layer DOS. A large peak in the surface LDOS located at the Fermi energy of the unrelaxed structure reveals the instability of this structure; this peak moves down to lower energy for the relaxed structure. The large relaxation of the surface atoms into the bulk region is attributed to the more localized nature of their 5*d* electrons, which weakens the *d*-*d* hybridization.

ACKNOWLEDGMENTS

This work was supported by the Korea Science and Engineering Foundation through Seoul National University Center for Theoretical Physics (SNU-CTP) and by the Office of Naval Research (under Grant No. N00014-94-l-0030).

[1] W. Moritz and D. Wolf, Surf. Sci. **163**, L655 (1985).
[2] E. C. Sowa, M. A. Van Hove, and D. L. Adams, Surf. Sci. **199**, 174 (1988).
[3] P. Fery, W. Moritz, and D. Wolf, Phys. Rev. B **38**, 7275 (1988).
[4] P. Fenter and T. Gustafsson, Phys. Rev. B **38**, 10 197 (1988).
[5] F. Masson and J. W. Rabalais, Surf. Sci. **253**, 245 (1991).
[6] M. Stock, J. Risse, U. Korte, and G. Meyer-Emsen, Surf. Sci. **233**, L243 (1990).
[7] E. Vlieg, I. K. Robinson, and K. Kern, Surf. Sci. **233**, 248 (1990).
[8] U. Korte and G. Meyer-Ehmsen, Surf. Sci. **271**, 616 (1992).
[9] S. M. Foiles, Surf. Sci. **191**, L779 (1987).
[10] M. Garofalo, E. Tosatti, and F. Ercolessi, Surf. Sci. **188**, 321 (1987).
[11] H. -J. Brocksch and K. H. Bennemann, Surf. Sci. **161**, 321 (1985).
[12] K. -M. Ho and K. P. Bohnen, Europhys. Lett. **4**, 345 (1987).
[13] M. Copel and T. Gustafsson, Phys. Rev. Lett. **57**, 723 (1986).
[14] S. Holmberg, H. C. Poon, Y. Jugnet, G. Grenet, and T. M. Duc, Surf. Sci. Lett. **254**, L475 (1991).
[15] M. S. Daw, Surf. Sci. **166**, L161 (1986).
[16] I. K. Robinson, Phys. Rev. Lett. **50**, 1145 (1985).
[17] L. D. Marks, Phys. Rev. Lett. **51**, 1000 (1983).
[18] S. Speller, S. Parascandola, and W. Heiland, Surf. Sci. **383**, 131 (1997).
[19] D. Tomanek, H. -J. Brocksch, and K. H. Bennemann, Surf. Sci. **318**, 243 (1994).
[20] E. Wimmer, H. Krakauer, M. Weinert, and A. J. Freeman, Phys. Rev. B **24**, 864 (1981).
[21] E. Wimmer, A. J. Freeman, and H. Krakauer, Phys. Rev. B **30**, 3113 (1984).
[22] C. Kittel, *Introduction to Solid State Physics* (Wiley, New York, 1996), p. 23.
[23] P. Hohenberg and W. Kohn, Phys. Rev. **136**, B864 (1964); W. Kohn and L. J. Sham, *ibid.* **140**, A1133 (1965), and references therein.
[24] L. Hedin and B. I. Lundqvist, J. Phys. C **4**, 2064 (1971).
[25] D. D. Koelling and B. N. Harmon, J. Phys. C **10**, 3107 (1977).
[26] W. Mannstadt and A. J. Freeman, Phys. Rev. B **55**, 13 298 (1997).
[27] C. G. Broyden, J. Inst. Math. Appl. **6**, 222 (1970).